Shaping the focal intensity distribution using spatial coherence

Thomas van Dijk,[1] Greg Gbur,[2] and Taco D. Visser[1,*]

[1]*Department of Physics and Astronomy, Free University, De Boelelaan 1081 HV, Amsterdam, The Netherlands*
[2]*Department of Physics and Optical Science, University of North Carolina at Charlotte, 9201 University City Boulevard, Charlotte, North Carolina 29223, USA*
**Corresponding author: tvisser@nat.vu.nl*

Received November 12, 2007; accepted December 11, 2007;
posted January 3, 2008 (Doc. ID 89423); published February 4, 2008

The intensity and the state of coherence are examined in the focal region of a converging, partially coherent wave field. In particular, Bessel-correlated fields are studied in detail. It is found that it is possible to change the intensity distribution and even to produce a local minimum of intensity at the geometrical focus by altering the coherence length. It is also shown that, even though the original field is partially coherent, in the focal region there are pairs of points at which the field is fully correlated and pairs of points at which the field is completely incoherent. The relevance of this work to applications such as optical trapping and beam shaping is discussed. © 2008 Optical Society of America

OCIS codes: 030.1640, 050.1960, 020.7010.

1. INTRODUCTION

Although light encountered under many practical circumstances is partially coherent, the intensity near focus of such wave fields has been studied in relatively few cases [1–5]. The correlation properties of focused partially coherent fields have been examined in [6,7], where it was shown that the correlation function exhibits phase singularities. In a recent study [8] it was suggested that the state of coherence of a field may be used to tailor the shape of the intensity distribution in the focal region. More specifically, it was shown that a minimum of intensity may occur at the geometrical focus.

In the present paper we explore converging, Bessel-correlated fields in more detail. Three-dimensional plots of the intensity distribution, in which the transition from a maximum of intensity to a minimum of intensity at the focal point can be seen, are presented. Also, the state of coherence of the field near focus is examined. It is found that there exist pairs of points at which the field is fully coherent and pairs at which the field is completely uncorrelated.

2. FOCUSING OF PARTIALLY COHERENT LIGHT

Consider first a converging, monochromatic field of frequency ω that emanates from a circular aperture with radius a in a plane screen (see Fig. 1). The origin O of the coordinate system is taken at the geometrical focus. The field at a point $Q(\mathbf{r}')$ on the wavefront A that fills the aperture is denoted by $U^{(0)}(\mathbf{r}',\omega)$. The field at an observation point $P(\mathbf{r})$ in the focal region is, according to the Huygens–Fresnel principle and within the paraxial approximation, given by the expression ([9], Chap. 8.8):

$$U(\mathbf{r},\omega) = -\frac{\mathrm{i}}{\lambda}\int_A U^{(0)}(\mathbf{r}',\omega)\frac{e^{\mathrm{i}ks}}{s}\mathrm{d}^2 r', \tag{1}$$

where $s=|\mathbf{r}-\mathbf{r}'|$ denotes the distance QP and λ is the wavelength of the field, and we have suppressed a time-dependent factor $\exp(-\mathrm{i}\omega t)$.

For a partially coherent wave, instead of just the field, one also has to consider the cross-spectral density function of the field at two points $Q(\mathbf{r}_1')$ and $Q(\mathbf{r}_2')$, namely,

$$W^{(0)}(\mathbf{r}_1',\mathbf{r}_2',\omega) = \langle U^*(\mathbf{r}_1',\omega)U(\mathbf{r}_2',\omega)\rangle, \tag{2}$$

where the angle brackets denote an ensemble average and the superscript (0) indicates fields in the aperture. This definition, as well as others related to coherence theory in the space-frequency domain, are discussed in ([10], Chaps. 4 and 5). On substituting from Eq. (1) into Eq. (2) we obtain for the cross-spectral density function in the focal region the formula

$$W(\mathbf{r}_1,\mathbf{r}_2,\omega) = \frac{1}{\lambda^2}\int\int_A W^{(0)}(\mathbf{r}_1',\mathbf{r}_2',\omega)\frac{e^{\mathrm{i}k(s_2-s_1)}}{s_1 s_2}\mathrm{d}^2 r_1'\mathrm{d}^2 r_2'. \tag{3}$$

The distances s_1 and s_2 are given by the expressions

$$s_1 = |\mathbf{r}_1 - \mathbf{r}_1'|, \tag{4}$$

$$s_2 = |\mathbf{r}_2 - \mathbf{r}_2'|. \tag{5}$$

If the Fresnel number of the focusing geometry is large compared to unity, i.e., if $N \equiv a^2/\lambda f \gg 1$, with f the radius of curvature of the field, then the distances s_1 and s_2 may be approximated by the expressions

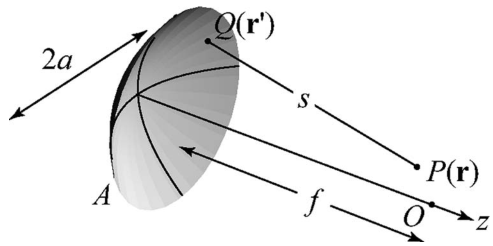

Fig. 1. Illustration of the notation.

$$s_1 \approx f - \mathbf{q}_1' \cdot \mathbf{r}_1, \tag{6}$$

$$s_2 \approx f - \mathbf{q}_2' \cdot \mathbf{r}_2, \tag{7}$$

where $\mathbf{q}_1'$ and $\mathbf{q}_2'$ are unit vectors in the directions $O\mathbf{r}_1'$ and $O\mathbf{r}_2'$, respectively. The factors s_1 and s_2 in the denominator of Eq. (3) may be approximated by f, and hence we obtain the expression

$$W(\mathbf{r}_1,\mathbf{r}_2,\omega) = \frac{1}{(\lambda f)^2}\int\int_A W^{(0)}(\mathbf{r}_1',\mathbf{r}_2',\omega) \times e^{ik(\mathbf{q}_1'\cdot\mathbf{r}_1 - \mathbf{q}_2'\cdot\mathbf{r}_2)}\mathrm{d}^2r_1'\mathrm{d}^2r_2'. \tag{8}$$

The spectral density of the focused field at a point of observation $P(\mathbf{r})$ in the focal region is given by the diagonal elements of the cross-spectral density function, i.e.,

$$S(\mathbf{r},\omega) = W(\mathbf{r},\mathbf{r},\omega). \tag{9}$$

From Eqs. (9) and (8) it follows that

$$S(\mathbf{r},\omega) = \frac{1}{(\lambda f)^2}\int\int_A W^{(0)}(\mathbf{r}_1',\mathbf{r}_2',\omega)e^{ik(\mathbf{q}_1'-\mathbf{q}_2')\cdot\mathbf{r}}\mathrm{d}^2r_1'\mathrm{d}^2r_2'. \tag{10}$$

A normalized measure of the field correlations is given by the spectral degree of coherence, which is defined as

$$\mu(\mathbf{r}_1,\mathbf{r}_2,\omega) \equiv \frac{W(\mathbf{r}_1,\mathbf{r}_2,\omega)}{[S(\mathbf{r}_1,\omega)S(\mathbf{r}_2,\omega)]^{1/2}}. \tag{11}$$

It may be shown that $0 \leqslant |\mu(\mathbf{r}_1,\mathbf{r}_2,\omega)| \leqslant 1$. The upper bound represents complete coherence of the field fluctuations at $\mathbf{r}_1$ and $\mathbf{r}_2$, whereas the lower bound represents complete incoherence. For all intermediate values the field is said to be partially coherent.

3. GAUSSIAN SCHELL-MODEL FIELDS

We now briefly review the focusing of a Gaussian Schell-model field with a uniform spectral density. Such a field is characterized by a cross-spectral density function of the form

$$W^{(0)}(\rho_1,\rho_2,\omega) = S^{(0)}(\omega)e^{-(\rho_2-\rho_1)^2/2\sigma_g^2}, \tag{12}$$

where $S^{(0)}(\omega)$ is the spectral density and σ_g a measure of the coherence length of the field in the aperture. Furthermore, $\boldsymbol{\rho}=(x,y)$ is the two-dimensional transverse vector that specifies the position of a point in the aperture plane. It was shown in [4] that the maximum of intensity always occurs at the geometrical focus, irrespective of the value of σ_g. Furthermore, the spectral density distribution was found to be symmetric about the focal plane and about the axis of propagation. On decreasing σ_g, the maximum spectral density decreases, and the secondary maxima and minima gradually disappear. In the coherent limit (i.e., $\sigma_g \to \infty$) the classical result [11] is retrieved.

The coherence properties of a focused Gaussian Schell-model field were examined in [6]. It was shown that the coherence length can be either larger or smaller than the width of the spectral density distribution. In addition, the spectral degree of coherence was found to possess phase singularities.

4. J_0-CORRELATED FIELDS

J_0-correlated fields with a constant spectral density are characterized by a cross-spectral density function of the form

$$W^{(0)}(\mathbf{r}_1',\mathbf{r}_2',\omega) = S^{(0)}(\omega)J_0(\beta|\mathbf{r}_2'-\mathbf{r}_1'|), \tag{13}$$

where J_0 denotes the Bessel function of the first kind of zeroth order. The correlation length is roughly given by β^{-1}. In [8] it was shown that the occurrence of a maximum of intensity at the geometrical focus is related to the positive definiteness of the cross-spectral density. Since the cross-spectral density function of Eq. (13) takes on negative values, another kind of behavior may now be possible. In this section we analyze the effect of the state of coherence on the three-dimensional spectral density distribution near focus. The cross-spectral density of the focused field is, according to Eq. (8), given by

$$W(\mathbf{r}_1,\mathbf{r}_2,\omega) = \frac{1}{(\lambda f)^2}\int\int_A S^{(0)}(\omega)J_0(\beta|\mathbf{r}_2'-\mathbf{r}_1'|) \times e^{ik(\mathbf{q}_1'\cdot\mathbf{r}_1-\mathbf{q}_2'\cdot\mathbf{r}_2)}\mathrm{d}^2r_1'\mathrm{d}^2r_2'. \tag{14}$$

We use scaled polar coordinates to write

$$\mathbf{r}_i' = (a\rho_i\cos\phi_i, a\rho_i\sin\phi_i, z_i) \qquad (i=1,2). \tag{15}$$

The spectral density is normalized to its value at the geometrical focus for a spatially fully coherent wave, i.e.,

$$S_{\mathrm{coh}} = \lim_{\beta\to 0} W(\mathbf{r}_1=\mathbf{r}_2=0,\omega) = \frac{a^4\pi^2 S^{(0)}(\omega)}{\lambda^2 f^2}. \tag{16}$$

To specify the position of an observation point we use the dimensionless Lommel variables, which are defined as

$$u = k\left(\frac{a}{f}\right)^2 z, \tag{17}$$

$$v = k\left(\frac{a}{f}\right)\rho = k(a/f)\sqrt{x^2+y^2}. \tag{18}$$

The expression for the normalized spectral density distribution is thus given by

$$S_{\text{norm}}(u,v,\omega)=\frac{S(u,v,\omega)}{S_{\text{coh}}}=\frac{1}{\pi^2}\int_0^{2\pi}\int_0^1\int_0^{2\pi}\int_0^1 \times J_0\{\beta a[\rho_1^2+\rho_2^2-2\rho_1\rho_2\cos(\phi_1-\phi_2)]^{1/2}\} \times\cos[v(\rho_1\cos\phi_1-\rho_2\cos\phi_2)+u(\rho_1^2-\rho_2^2)/2] \times\rho_1\rho_2 \mathrm{d}\rho_1\mathrm{d}\phi_1\mathrm{d}\rho_2\mathrm{d}\phi_2. \tag{19}$$

It can be shown that this distribution is symmetric about the plane $u=0$ and the line $v=0$. To reduce this four-dimensional integral to a sum of two-dimensional integrals we use a coherent mode expansion, as described in Appendix A.

The contours and three-dimensional images of the spectral density of a converging J_0-correlated Schell-model field are shown for several values of the coherence length β^{-1} in Figs. 2–4. When this length is significantly larger than the aperture size a, the intensity pattern of the field in the focal region approaches that of the coherent case of [11]. This is illustrated in Fig. 2, where $(\beta a)^{-1}=2$. This quantity is a measure of the effective coherence of the field in the aperture.

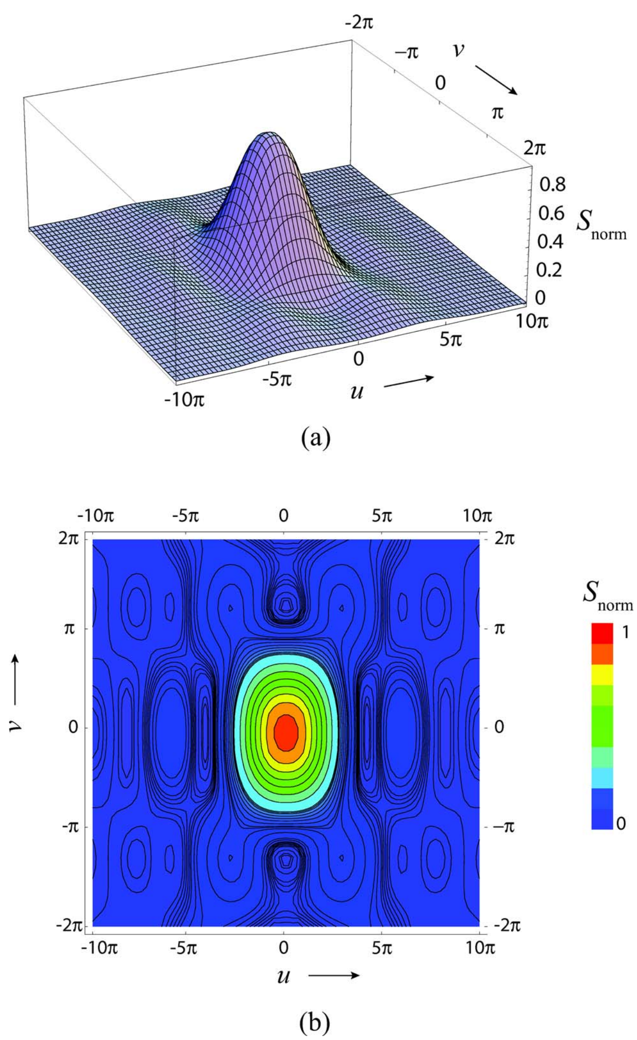

Fig. 2. (Color online) (a) Three-dimensional normalized spectral density distribution and (b) its contours for the case $\beta^{-1}=0.02$ m, $a=0.01$ m and hence $(\beta a)^{-1}=2.00$. In this example $\lambda=500$ nm, and $f=2$ m.

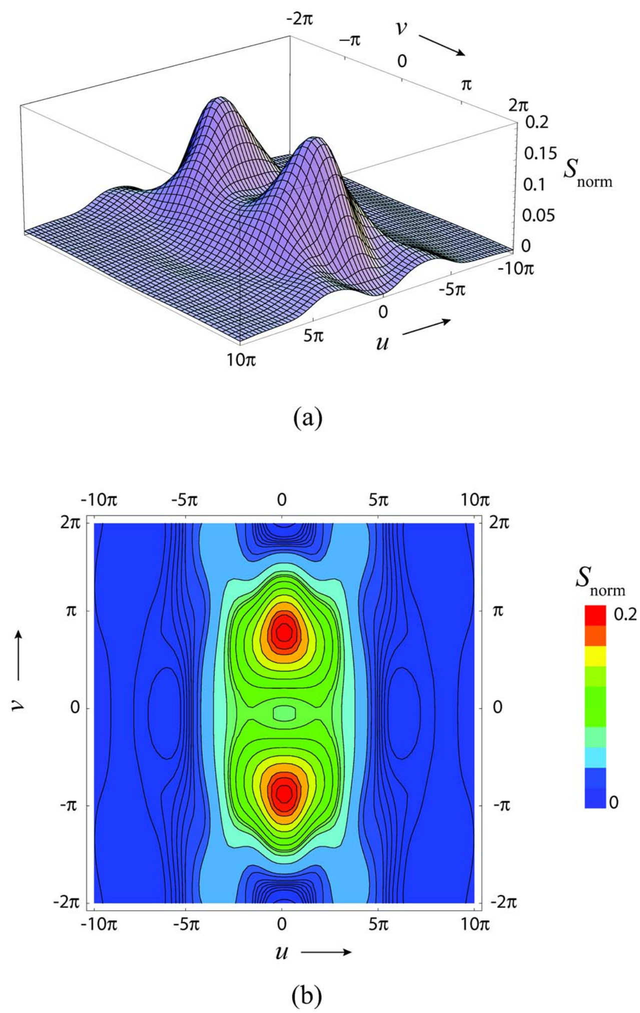

Fig. 3. (Color online) (a) Three-dimensional normalized spectral density distribution and (b) its contours for the case $\beta^{-1}=3.5\times10^{-3}$ m, $a=0.01$ m and hence $(\beta a)^{-1}=0.35$. The other parameters are the same as those of Fig. 2.

When the correlation length is decreased, a local minimum appears at the geometrical focus. This is shown in Fig. 3 for the case $(\beta a)^{-1}=0.35$. An intensity minimum can be seen at $u=v=0$. Also, the overall intensity has decreased.

Figure 4 shows the intensity pattern for the case $(\beta a)^{-1}=0.25$. The minimum at the geometrical focus is now deeper, the focal spot is broadened, and the overall intensity has decreased even further.

The behavior of the cross-spectral density function of the field in the aperture for the cases mentioned above is shown in Fig. 5. The spectral degree of coherence is plotted as a function of $\rho=|\mathbf{r}_2-\mathbf{r}_1|$. It is to be noted that for the two cases in which the spectral density has a local minimum at the geometrical focus, the spectral degree of coherence also takes on negative values.

5. SPATIAL CORRELATION PROPERTIES

We next turn our attention to the spectral degree of coherence in the focal region of a J_0-correlated Schell model field. We first look at pairs of points on the z-axis, i.e.,

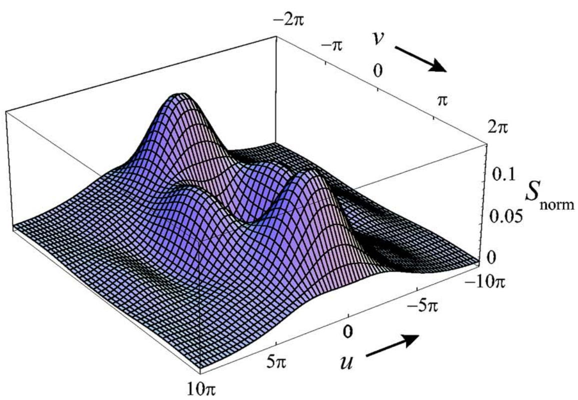

(a)

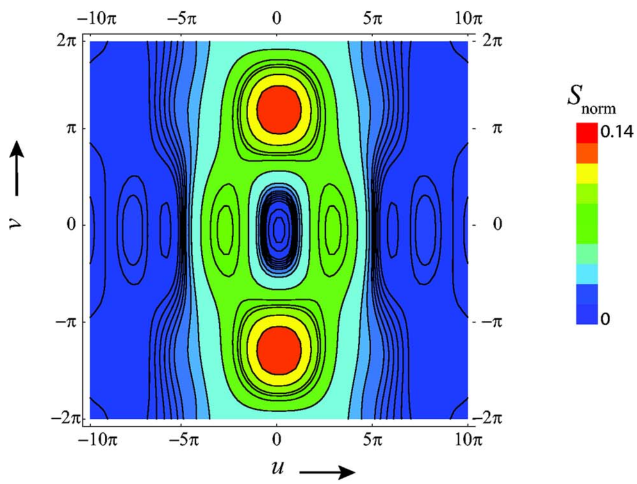

(b)

Fig. 4. (Color online) (a) Three-dimensional normalized spectral density distribution and (b) its contours for the case $\beta^{-1}=2.5\times10^{-3}$ m, $a=0.01$ m and hence $(\beta a)^{-1}=0.25$. The other parameters are the same as those of Fig. 2.

$$\mathbf{r}_1=(0,0,z_1), \tag{20}$$

$$\mathbf{r}_2=(0,0,z_2). \tag{21}$$

On using cylindrical coordinates ρ and ϕ and the expressions in [6] we obtain

$$\mathbf{q}_1'\cdot\mathbf{r}_1\approx-z_1(1-\rho_1^2/2f^2), \tag{22}$$

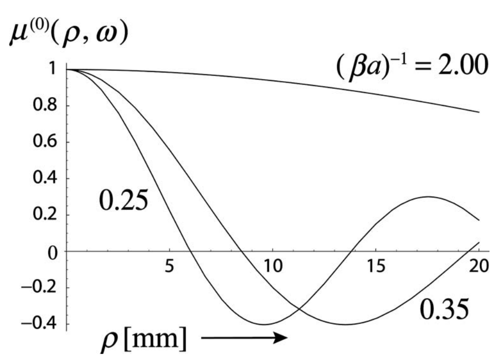

Fig. 5. Spectral degree of coherence of the field in the aperture $\mu^{(0)}(\boldsymbol{\rho},\omega)$ for three different values of $(\beta a)^{-1}$, as discussed in the text. In this example $\lambda=500$ nm, $a=0.01$ m, and $f=2$ m.

$$\mathbf{q}_2'\cdot\mathbf{r}_2\approx-z_2(1-\rho_2^2/2f^2). \tag{23}$$

Substituting these approximations in Eq. (14), we obtain for the cross-spectral density the expression

$$W(0,0,z_1;0,0,z_2;\omega)=\frac{1}{(\lambda f)^2}\int_0^{2\pi}\int_0^a\int_0^{2\pi}\int_0^a S^{(0)}(\omega)\times J_0\{\beta[\rho_1^2+\rho_2^2-2\rho_1\rho_2\cos(\phi_1-\phi_2)]^{1/2}\}\times e^{ik[-z_1(1-\rho_1^2/2f^2)+z_2(1-\rho_2^2/2f^2)]}\rho_1\rho_2\times\mathrm{d}\phi_1\mathrm{d}\rho_1\mathrm{d}\phi_2\mathrm{d}\rho_2. \tag{24}$$

As shown in Appendix A, the coherent mode expansion for J_0 reads

$$J_0\{\beta[\rho_1^2+\rho_2^2-2\rho_1\rho_2\cos(\phi_1-\phi_2)]^{1/2}\}=J_0(\beta\rho_1)J_0(\beta\rho_2)+\sum_{n=1}^{\infty}2[J_n(\beta\rho_1)J_n(\beta\rho_2)\cos[n(\phi_1-\phi_2)]]. \tag{25}$$

It is to be noted that in the expression for the cross-spectral density, Eq. (24), the angular dependence resides exclusively in the correlation function; hence after integration over ϕ_1 and ϕ_2 only the zeroth-order term of Eq. (25) remains. We therefore find that

$$W(0,0,z_1;0,0,z_2;\omega)=f^*(0,0,z_1;\omega)f(0,0,z_2;\omega), \tag{26}$$

with

$$f(0,0,z;\omega)=\frac{k}{f}\int_0^a J_0(\beta\rho)e^{ikz(1-\rho^2/2f^2)}\rho\mathrm{d}\rho. \tag{27}$$

From this result and Eq. (11) it readily follows that

$$|\mu(0,0,z_1;0,0,z_2;\omega)|=1. \tag{28}$$

This implies that the field is fully coherent for all pairs of points along the z axis, even though the field in the aperture is partially coherent. This surprising effect can be understood by noticing that only a single coherent mode comes into play.

Next we examine pairs of points that lie in the focal plane. One point is taken to be at the geometrical focus O. Due to the rotational invariance of the system, we may assume, without loss of generality, that the second point lies on the x axis. Hence we consider pairs of points for which

$$\mathbf{r}_1=(0,0,0), \tag{29}$$

$$\mathbf{r}_2=(x,0,0). \tag{30}$$

The cross-spectral density, Eq. (14), then yields

$$W(0,0,0;x,0,0;\omega)=\frac{1}{(\lambda f)^2}\int_0^{2\pi}\int_0^a\int_0^{2\pi}\int_0^a S^{(0)}(\omega)\times J_0\{\beta[\rho_1^2+\rho_2^2-2\rho_1\rho_2\cos(\phi_1-\phi_2)]^{1/2}\}\times e^{-ik(\rho_2 x\cos\phi_2)/f}\rho_1\rho_2\mathrm{d}\phi_1\mathrm{d}\rho_1\mathrm{d}\phi_2\mathrm{d}\rho_2. \tag{31}$$

On using the coherent mode expansion of J_0 and integrating over ϕ_1, again a single term remains, i.e.,

$$W(0,0,0;x,0,0;\omega) = \frac{2\pi}{(\lambda f)^2}\int_0^a \int_0^{2\pi} \int_0^a S^{(0)}(\omega) J_0(\beta\rho_1) J_0(\beta\rho_2) \times \cos\left(k\frac{\rho_2 x}{f}\cos\phi_2\right)\rho_1\rho_2 \mathrm{d}\rho_1 \mathrm{d}\phi_2 \mathrm{d}\rho_2. \tag{32}$$

It is to be noted that this expression is real-valued.

In order to obtain the spectral degree of coherence, we use the facts that

$$S(0,0,0;\omega) = \left(\frac{k}{f}\right)^2 \int_0^a \int_0^a J_0(\beta\rho_1) J_0(\beta\rho_2)\rho_1\rho_2 \mathrm{d}\rho_1 \mathrm{d}\rho_2 \tag{33}$$

and

$$S(x,0,0;\omega) = \frac{1}{(\lambda f)^2}\int_0^{2\pi}\int_0^a \int_0^{2\pi} \int_0^a S^{(0)}(\omega) \times J_0\{\beta[\rho_1^2+\rho_2^2-2\rho_1\rho_2\cos(\phi_1-\phi_2)]^{1/2}\} \times \cos[kx(\rho_1\cos\phi_1-\rho_2\cos\phi_2)/f]\rho_1\rho_2 \times \mathrm{d}\phi_1 \mathrm{d}\rho_1 \mathrm{d}\phi_2 \mathrm{d}\rho_2. \tag{34}$$

Examples of the spectral degree of coherence $\mu(0,0,0;x,0,0;\omega)$ are depicted in Figs. 6 and 7 for selected values of the coherence parameter $(\beta a)^{-1}$. For comparison's sake the normalized spectral density is also shown. In Fig. 6(a) two regions can be distinguished, regions where the fields are approximately co-phasal [i.e., $\mu(0,0,0;x,0,0;\omega)\approx 1$] and regions where the fields have opposite phases [i.e., $\mu(0,0,0;x,0,0;\omega)\approx -1$]. In between these two regions the spectral degree of coherence exhibits phase singularities [i.e., $\mu(0,0,0;x,0,0;\omega)=0$]. The latter points coincide with approximate zeros of the field.

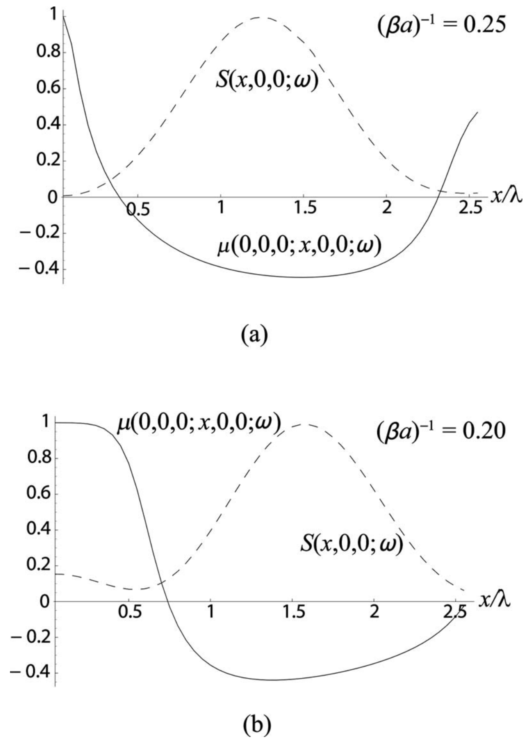

Fig. 7. Spectral degree of coherence $\mu(0,0,0;x,0,0;\omega)$ (solid curve) and the spectral density $S(x,0,0,\omega)$ normalized to its maximum value (dashed curve), for the case (a), $(\beta a)^{-1}=0.25$ and (b), $(\beta a)^{-1}=0.2$. In this example $\lambda=0.6328$ μm, $a=0.01$ m, and $f=0.02$ m.

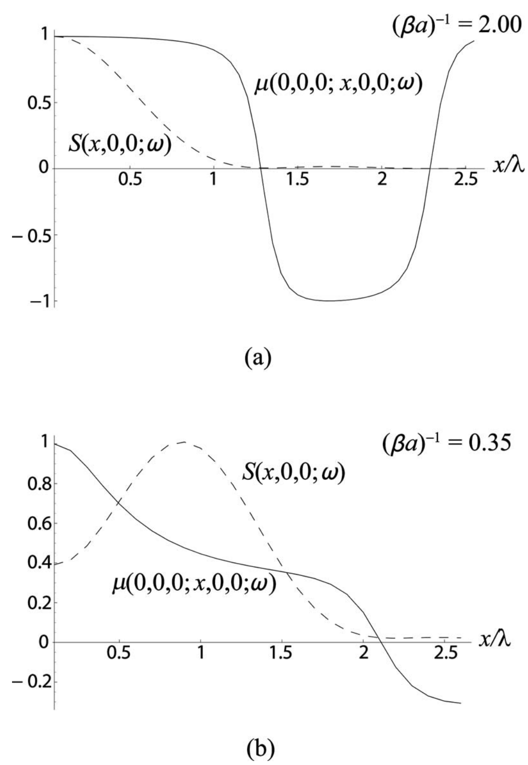

Fig. 6. Spectral degree of coherence $\mu(0,0,0;x,0,0;\omega)$ (solid curve) and spectral density $S(x,0,0,\omega)$ normalized to its maximum value (dashed curve) for the case (a), $(\beta a)^{-1}=2$ and (b), $(\beta a)^{-1}=0.35$. In this example $\lambda=0.6328$ μm, $a=0.01$ m, and $f=0.02$ m.

When the coherence parameter is decreased, the overall intensity gets lower. This is shown in Fig. 6(b) for the case $(\beta a)^{-1}=0.35$. An intensity minimum now occurs at the geometrical focus. The spectral degree of coherence still possesses a phase singularity; however its position no longer coincides with a zero of the field.

On further decreasing the coherence, the spectral density at focus almost reaches zero. This is shown in Fig. 7(a) for the case $(\beta a)^{-1}=0.25$. The spectral density rises again if the correlation parameter is decreased further, as can been seen in Fig. 7(b). In all cases the spectral degree of coherence exhibits phase singularities.

6. OTHER CORRELATION FUNCTIONS

In this section we examine the spectral density in the focal plane for other Bessel-correlated fields. In particular we consider a cross-spectral density function of the form (see Section 5.3 of [10])

$$W_n^{(0)}(\boldsymbol{\rho}_1,\boldsymbol{\rho}_2,\omega) = S^{(0)}(\omega)2^{n/2}\Gamma\left(1+\frac{n}{2}\right)\frac{J_{n/2}(\beta|\boldsymbol{\rho}_2-\boldsymbol{\rho}_1|)}{(\beta|\boldsymbol{\rho}_2-\boldsymbol{\rho}_1|)^{n/2}}, \tag{35}$$

where $J_{n/2}$ is a Bessel function of the first kind and Γ is the gamma function. The case $n=0$ was discussed in the previous sections.

Let us denote a position in the focal plane with the vector $(\rho,0)$. The spectral density is then given by the expression

$$S_n(\boldsymbol{\rho},0,\omega) = \frac{1}{(\lambda f)^2}\int_A\int_A W_n^{(0)}(\boldsymbol{\rho}_1,\boldsymbol{\rho}_2,\omega)e^{-ik(\boldsymbol{\rho}_2-\boldsymbol{\rho}_1)\cdot\boldsymbol{\rho}/f}\mathrm{d}^2\rho_1\mathrm{d}^2\rho_2. \tag{36}$$

This can be simplified to [12]

$$S_n(\boldsymbol{\rho},0,\omega) = 2\left(\frac{ka^2}{f}\right)^2\int_0^1 C(b)W_n^{(0)}(2a\beta b)J_0\left(\frac{2ka\rho b}{f}\right)b\mathrm{d}b, \tag{37}$$

where

$$C(b) = (2/\pi)[\arccos(b) - b(1-b^2)^{1/2}]. \tag{38}$$

As before, the spectral density is normalized to its value for a fully coherent field at the geometrical focus. The normalized spectral density is thus given by the formula

$$\frac{S_n(\boldsymbol{\rho},0,\omega)}{S_{\mathrm{coh}}} = \frac{8}{S^{(0)}(\omega)}\int_0^1 C(b)W_n^{(0)}(2a\beta b)J_0\left(\frac{2ka\rho b}{f}\right)b\mathrm{d}b. \tag{39}$$

An example is shown Fig. 8 for the case $n=2$ and $(\beta a)^{-1}=0.13$. It is seen that the spectral density now has a flat-topped profile. Fields with such a $J_1(x)/x$ correlation can be synthesized by placing a circular incoherent source in the first focal plane of a converging lens [13].

7. CONCLUSIONS

We have investigated the behavior of selected Bessel-correlated, focused fields. It is observed that J_0-correlated fields produce a tunable, local minimum of intensity within a high-intensity shell of light. This observation suggests that such beams might be useful in a number of optical manipulation applications. In particular, it is well appreciated that optical trapping of high-index particles requires high intensity at focus, while the trapping of low-index particles requires low intensity at focus. The J_0 focusing configuration allows one to construct a system that can continuously switch between these two trapping conditions [14].

It is also observed that $J_1(x)/x$ correlated fields result in a flat-top intensity distribution. Such an intensity distribution could be useful in applications where a uniform intensity spot is required, such as lithography.

These intensity distributions, and others, can be roughly predicted using straightforward Fourier optics. The image that appears in the focal plane is essentially the Fourier transform of the aperture-truncated correlation function in the lens plane. This correlation function can in turn be generated by an incoherent source whose aperture is given by the Fourier transform of the correlation function. One such example is using an annular incoherent source to produce a J_0-correlated field at the lens. The detailed three-dimensional structure of the light field in the focal region, however, requires a numerical solution of the diffraction problem.

It is important to note that this method of generating the necessary correlations is by no means unique. Any technique that produces the desired Bessel correlation in the lens plane will result in the same intensity distribution at focus. For instance, one could use a coherent laser field transmitted through a rotating ground-glass plate with the desired correlations.

This coherence shaping of the intensity distribution at focus holds promise as a new technique for optical manipulation [c.f. [15]].

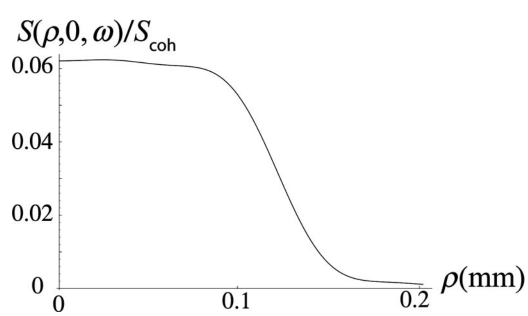

Fig. 8. Normalized spectral density, Eq. (39), in the focal plane for the case $(\beta a)^{-1}=0.13$. In this example $\lambda=500$ nm, $a=0.01$ m, $n=2$, and $f=2$ m.

APPENDIX A: COHERENT-MODE EXPANSION OF A J_0-CORRELATED FIELD

Following Gori et al. [16], we use the coherent mode expansion for the cross-spectral density function given by Eq. (13) to evaluate expression (19). Since it belongs to the Hilbert–Schmidt class, it can be expressed in the form [17]

$$W^{(0)}(\boldsymbol{\rho}_1,\boldsymbol{\rho}_2,\omega) = \sum_n \lambda_n(\omega)\psi_n^*(\boldsymbol{\rho}_1,\omega)\psi_n(\boldsymbol{\rho}_2,\omega). \tag{A.1}$$

Here $\psi_n(\boldsymbol{\rho},\omega)$ are the orthonormal eigenfunctions and $\lambda_n(\omega)$ the eigenvalues of the integral equation

$$\int_D W^{(0)}(\boldsymbol{\rho}_1,\boldsymbol{\rho}_2,\omega)\psi_n(\mathbf{r}_1,\omega)\mathrm{d}^2\rho_1 = \lambda_n(\omega)\psi_n(\boldsymbol{\rho}_2,\omega), \tag{A.2}$$

where the integral extends over the aperture plane D. We rewrite the expansion (A.1) as

$$W^{(0)}(\boldsymbol{\rho}_1,\boldsymbol{\rho}_2,\omega) = \sum_n \lambda_n(\omega)W_n(\boldsymbol{\rho}_1,\boldsymbol{\rho}_2,\omega), \tag{A.3}$$

where $W_n(\boldsymbol{\rho}_1,\boldsymbol{\rho}_2,\omega)=\psi_n^*(\boldsymbol{\rho}_1,\omega)\psi_n(\boldsymbol{\rho}_2,\omega)$. The spectral degree of coherence corresponding to a single term, W_n, is clearly unimodular. Hence the expansion in Eq. (A.3) represents the cross-spectral density as a superposition of fully coherent modes.

In the case of a J_0-correlated field the expression for the eigenfunctions $\psi_n(\boldsymbol{\rho},\omega)$ reads [16]

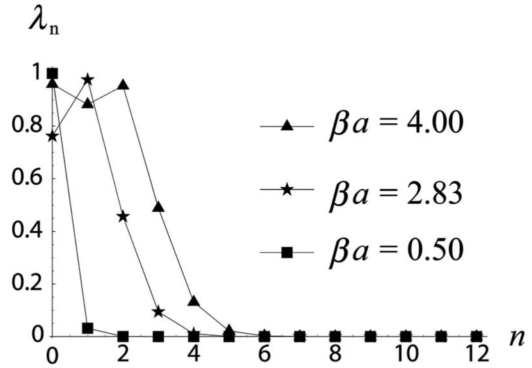

Fig. 9. Eigenvalues λ_n versus n for a J_0-correlated field with a uniform spectral density across the plane of the aperture. Only the points corresponding to integer values of n are meaningful; the connecting lines are drawn to aid the eye.

$$\psi_n(\rho,\phi) = C_n\sqrt{S^{(0)}(\omega)}[a_n J_n(\beta\rho)e^{-\mathrm{i}n\phi} + b_n J_{-n}(\beta\rho)e^{\mathrm{i}n\phi}], \quad (A.4)$$

where C_n is a suitable normalization factor and the ratio a_n/b_n is arbitrary. On substituting from Eq. (A.4) into Eq. (A.2) and using Neumann's addition theorem

$$J_0\{\beta[\rho_1^2+\rho_2^2-2\rho_1\rho_2\cos(\phi_1-\phi_2)]^{1/2}\} = \sum_{k=-\infty}^{\infty} J_k(\beta\rho_1)J_k(\beta\rho_2)e^{\mathrm{i}k(\phi_1-\phi_2)}, \quad (A.5)$$

we find that the eigenvalues λ_n are given by the formulas

$$\lambda_n = \pi a^2 S^{(0)}(\omega)[J_n^2(\beta a) - J_{n-1}(\beta a)J_{n+1}(\beta a)], \quad (n=0,1,2,\ldots). \quad (A.6)$$

To ensure that all the functions $\psi_n(\boldsymbol{\rho},\omega)$ are orthonormal, we may choose

$$C_n = \frac{1}{\sqrt{\lambda_n}} \qquad (n=0,1,2,\ldots). \quad (A.7)$$

This choice implies that

$$(a_0+b_0)^2 = 1 \quad (A.8)$$

$$a_n^2+b_n^2 = 1 \qquad (n=1,2,3,\ldots). \quad (A.9)$$

Hence we find a twofold degeneracy for the eigenfunctions ψ_n except for the case that $n=0$. We thus obtain the expansion

$$J_0\{\beta[\rho_1^2+\rho_2^2-2\rho_1\rho_2\cos(\phi_1-\phi_2)]^{1/2}\} = J_0(\beta\rho_1)J_0(\beta\rho_2) + \sum_{n=1}^{\infty} 2\{J_n(\beta\rho_1)J_n(\beta\rho_2) \times\cos[n(\phi_1-\phi_2)]\}, \quad (A.10)$$

where we have used the fact that the functions J_n and J_{-n} are related by [18]

$$J_{-n}(x) = (-1)^n J_n(x) \qquad (n\in\mathbb{N}). \quad (A.11)$$

The behavior of the eigenvalues λ_n versus n is shown in Fig. 9. Although the decreasing behavior of the eigenvalues is not strictly monotonic it can be seen that as soon n exceeds βa the eigenvalues become very small. In other words, only those modes whose index n is smaller than βa contribute effectively to the cross-spectral density.

REFERENCES

1. B. Lü, B. Zhang, and B. Cai, "Focusing of a Gaussian Schell-model beam through a circular lens," J. Mod. Opt. **42**, 289–298 (1995).
2. W. Wang, A. T. Friberg, and E. Wolf, "Focusing of partially coherent light in systems of large Fresnel numbers," J. Opt. Soc. Am. A **14**, 491–496 (1997).
3. A. T. Friberg, T. D. Visser, W. Wang, and E. Wolf, "Focal shifts of converging diffracted waves of any state of spatial coherence," Opt. Commun. **196**, 1–7 (2001).
4. T. D. Visser, G. Gbur, and E. Wolf, "Effect of the state of coherence on the three-dimensional spectral intensity distribution near focus," Opt. Commun. **213**, 13–19 (2002).
5. L. Wang and B. Lü, "Propagation and focal shift of J_0-correlated Schell-model beams," Optik (Stuttgart) **117**, 167–172 (2006).
6. D. G. Fischer and T. D. Visser, "Spatial correlation properties of focused partially coherent light," J. Opt. Soc. Am. A **21**, 2097–2102 (2004).
7. L. Rao and J. Pu, "Spatial correlation properties of focused partially coherent vortex beams," J. Opt. Soc. Am. A **24**, 2242–2247 (2007).
8. G. Gbur and T. D. Visser, "Can spatial coherence effects produce a local minimum of intensity at focus?" Opt. Lett. **28**, 1627–1629 (2003).
9. M. Born and E. Wolf, *Principles of Optics*, 7th ed. (expanded) (Cambridge Univ. Press, 1999).
10. L. Mandel and E. Wolf, *Optical Coherence and Quantum Optics* (Cambridge Univ. Press, 1995).
11. E. H. Linfoot and E. Wolf, "Phase distribution near focus in an aberration-free diffraction image," Proc. Phys. Soc. London, Sect. B **69**, 823–832 (1956).
12. J. T. Foley, "Effect of an aperture on the spectrum of partially coherent light," J. Opt. Soc. Am. A **8**, 1099–1105 (1991).
13. E. Wolf and D. F. V. James, "Correlation-induced spectral changes," Rep. Prog. Phys. **59**, 771–818 (1996).
14. K. T. Gahagan and G. A. Swartzlander, Jr., "Simultaneous trapping of low-index and high-index microparticles observed with an optical-vortex trap," J. Opt. Soc. Am. B **16**, 533–537 (1999).
15. J. Arlt and M. J. Padgett, "Generation of a beam with a dark focus surrounded by regions of higher intensity: the optical bottle beam," Opt. Lett. **25**, 191–193 (2000).
16. F. Gori, G. Guattari, and C. Padovani, "Modal expansion for J_0-correlated Schell-model sources," Opt. Commun. **4**, 311–316 (1987).
17. E. Wolf, "New theory of partial coherence in the space-frequency domain. Part I: spectra and cross spectra of steady-state sources," J. Opt. Soc. Am. **72**, 343–351 (1982).
18. G. B. Arfken and H. J. Weber, *Mathematical Methods for Physicists*, 5th ed. (Academic, 2001).